IL NUOVO CIMENTO **41 C** (2018) 120
DOI 10.1393/ncc/i2018-18120-x

COMMUNICATIONS: SIF Congress 2017

The central region of the test bench cyclotron for the IsoDAR experiment

G. D'AGOSTINO([1])([2]) on behalf of the IsoDAR COLLABORATION

([1]) *Istituto Nazionale di Fisica Nucleare, Laboratori Nazionali del Sud - Catania, Italy*
([2]) *Dipartimento di Fisica e Astronomia, Università degli Studi di Catania - Catania, Italy*

received 31 January 2018

Summary. — The IsoDAR experiment proposes the construction of a cyclotron to accelerate a 5 mA H_2^+ beam up to 60 A MeV to investigate the existence of sterile neutrinos. Due to the high beam current and the serious space charge effects, the beam injection and the central region are challenging items for this cyclotron. For this reason, a 1 A MeV test bench cyclotron will be built. In this paper, the simulation study for the spiral inflector and early turns of beam acceleration in the central region of the test bench cyclotron will be presented.

1. – Introduction

The interest of the scientific community on neutrino physics is growing through the years. The mass hierarchy problem and the existence of sterile neutrinos are currently open questions. IsoDAR (Isotope Decay At Rest) is an experimental project, proposed by MIT (Massachusetts Institute of Technology), to search for the existence of sterile neutrinos by measuring the disappearance of electron antineutrinos produced by isotope decay at rest [1]. Furthermore, IsoDAR aims at an accurate measurement of the $\bar{\nu}_e - e$ scattering and also looks for the production and decay of exotic particles [2].

In the IsoDAR experiment, a 10 mA proton beam will be directed onto a ^{9}Be target producing a high neutron flux. Then, the neutrons will enter a 99.99% isotopically pure ^{7}Li sleeve, surrounding the target. The neutrons capture by ^{7}Li isotopes will create great quantities of ^{8}Li, which will produce electron antineutrinos by beta decay. The $\bar{\nu}_e$ will be detected via IBD (Inverse Beta Decay), $\bar{\nu}_e + p \rightarrow e^+ + n$, using KamLAND, an underground kiloton-scale liquid scintillator detector characterized by high efficiency inverse-beta-decay identification capability [3]. A sketch of the IsoDAR experiment is shown in fig. 1.

In order to have high statistics in a few years, a substantial antineutrino flux is required and, consequently, a high proton beam current must be generated and accelerated. The primary beam, used for the electron antineutrinos production, will be delivered by a 4-fold

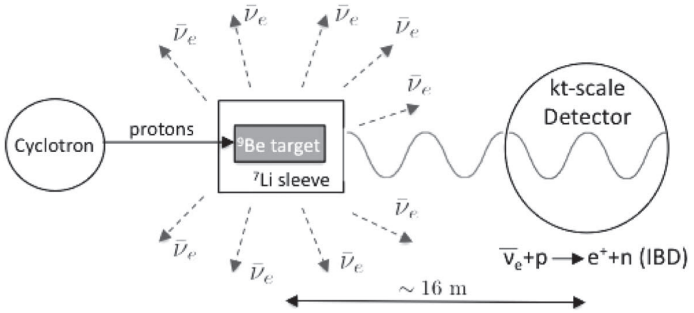

Fig. 1. – Schematic view (not in scale) of the IsoDAR experiment.

symmetric cyclotron accelerating a 5 mA H_2^+ beam up to the energy of 60 A MeV. The beam will be extracted by means of an electrostatic deflector and the H_2^+ ions stripped into protons outside the accelerating machine.

The project poses ambitious goals, which require innovative technical solutions for different issues. In particular, one of the main key-points for the success of the project is the generation, transport and acceleration of a high H_2^+ beam current.

Since the typical acceptance of an unbunched beam into RF buckets is of the order of 10%, the ion source should provide up to 50 mA of H_2^+. This value is challenging for present H_2^+ ion sources [4, 5]. However, the beam pre-bunching before the cyclotron injection should allow reducing the required H_2^+ current of about a factor two, down to 25 mA. Anyway, this H_2^+ beam current value is not easily reachable at the present stage of plasma-based ion sources. MIST-1, a dedicated H_2^+ multicusp ion source for IsoDAR, is currently being developed and tested at MIT [6,7]. In addition, a RFQ (Radio Frequency Quadrupole) is now being designed to be used to pre-accelerate, bunch and focus the beam before the cyclotron injection. The use of a RFQ in place of a typical LEBT (Low Energy Beam Transport) system should increase the beam capture efficiency in the cyclotron to a value $> 40\%$ [7, 8].

The H_2^+ beam will be axially injected into the cyclotron through a spiral inflector [9]. The injection system and cyclotron design requires particular attention since, due to the high beam current, the space charge effects are not negligible and affect negatively the beam behaviour, especially at low energy.

An injection and acceleration test will be performed to characterize the new ion source, the low energy beam transport, the RFQ and the IsoDAR cyclotron central region including the spiral inflector. For this reason, a 1 A MeV test bench cyclotron is being designed, including the spiral inflector and central region. In this paper, the preliminary results of the simulations on the spiral inflector and central region of the IsoDAR test bench cyclotron, performed in collaboration with IBA (Ion Beam Applications) company, are presented.

2. – Design of the central region

The design of the spiral inflector and central region of the IsoDAR test bench cyclotron is constrained by requirements related to the full cyclotron:

1) injected particles (ion charge to mass ratio, injection energy, energy spread introduced by the RFQ);

TABLE I. – *IsoDAR cyclotron and injected particles parameters to be considered as constraints during the injection system study.*

Ion charge to mass ratio	0.5	Injection energy	35 AkeV
Energy spread	$\pm$ 2% E_{inj}	Maximum energy	1 A MeV
Pole radius	370 mm	Hill gap	60 mm
Valley gap	600 mm	Number of RF cavities	4
Dee angle	36°	RF harmonic mode	4th
RF frequency	32.8 MHz	RF voltage	70 kV

2) magnetic structure (magnetic field level and shape in the cyclotron centre);

3) accelerating structure (number of dees, dee voltage, RF frequency, harmonic accelerating mode).

The magnetic structure has been already designed at INFN-LNS Catania in the past months. The test bench cyclotron has a pole radius equal to 370 mm and is able to accelerate the H_2^+ beam up to the energy of 1 A MeV. The H_2^+ ions can perform only a few turns in the test bench cyclotron due to the small sizes of the machine. A 60 mm vertical gap is adopted in order to improve the transmission of high beam current. Table I contains the IsoDAR cyclotron and injected particles parameters to be considered as constraints in the injection system study. The geometrical space available for the spiral inflector and central region electrodes in the cyclotron centre is a further constraint to be taken into account.

In addition, the injection system for the IsoDAR test bench cyclotron must be developed to fulfil the following design goals [10]:

1) horizontal centering of the beam with respect to the cyclotron centre;

2) vertical centering of the beam with respect to the median plane;

3) matching of the beam phase space with respect to the cyclotron eigenellipse;

4) vertical focusing;

5) minimization of beam losses;

6) good longitudinal acceptance;

7) turn separation.

The achievement of the above-mentioned goals is not easy because of space charge effects produced by the high beam current required by IsoDAR. The Coulomb forces between the charged particles create a self-field which acts on the particles, leading to the beam blow-up and defocusing in both transverse planes. Moreover, the space charge effects induce energy spread with possible loss of the turn separation. These effects are generally proportional to the beam intensity [11].

In the case of the IsoDAR cyclotron, the use of a numerical code, as AOC (Advanced Orbit Code) [12], taking into account the space charge effects, is mandatory for the correct evaluation of the beam dynamics, especially for the design of the low energy region. This approach allows to estimate the vertical losses in the central region as well

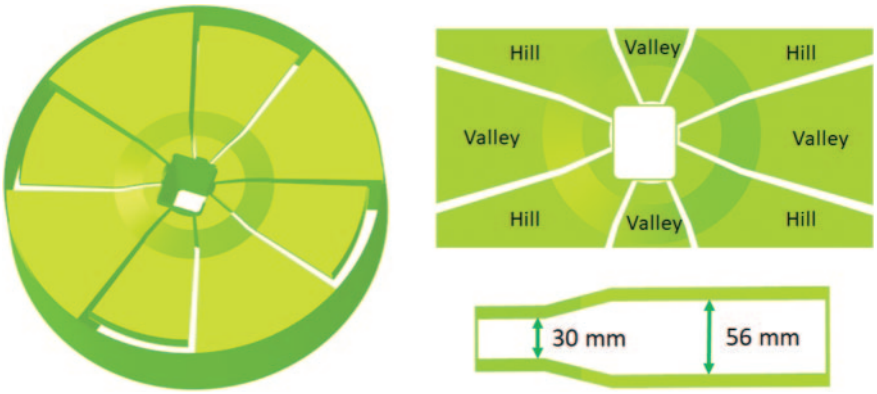

Fig. 2. – 3D model of the central region of the IsoDAR test bench cyclotron. Dee-tips have two vertical apertures equal to 30 mm at the cyclotron centre and 56 mm at the larger radii.

as the beam radial size along the whole path in the machine, since the beam extraction from the IsoDAR cyclotron will be through an electrostatic deflector.

The following approach is being used to design the injection system for the IsoDAR test bench cyclotron:

1) extraction of the B-field in and around the inflector volume and in the median plane from the Opera-3d [13] model of the IsoDAR test bench cyclotron magnet;

2) realization of a first crude Opera-3d model of the central region and step by step refinement. Individuation of the injection point in the central region and of the accelerating gaps such that the reference orbit is centred with respect to the cyclotron centre and its RF phase is centred with respect to the accelerating wave (isochronism). Simulation of the forward orbit tracking from the 70 keV injection energy towards the permitted maximum energy;

3) calculation of a preliminary inflector central orbit, passing through the injection point. For this purpose, AOC code simulates the spiral inflector by an electric field that is always perpendicular to the orbit. An automatic iteration optimizes the inflector parameters such that the orbit is injected perfectly onto the median plane and also perfectly on the accelerated equilibrium orbit;

4) design of the real 3D inflector electrodes around the estimated central orbit using Opera-3d;

5) design test by orbit tracking in the real 3D electric and magnetic fields, including small modifications to the spiral inflector if needed.

Figure 2 shows a 3D view of the Opera-3d central region model that has been obtained. The vertical aperture of the central region electrodes is not equal everywhere. Dee-tips have a vertical aperture equal to 30 mm at the first turn and 56 mm at the other turns. The smallest vertical gap at the inner cyclotron radii has been arbitrarily chosen to mitigate the transit time factor effects on the beam dynamics in the first turn. A copper housing, which surrounds the spiral inflector, allows for avoiding the interaction between the RF cavities electric fields and the inflector electric field. Furthermore, a copper

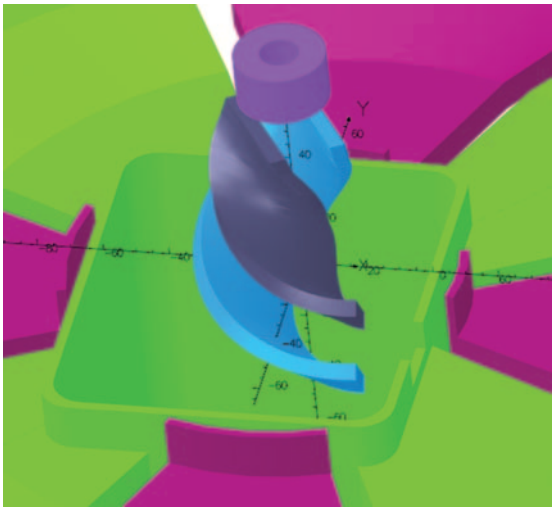

Fig. 3. – 3D view of the spiral inflector of the IsoDAR test bench cyclotron. The collimator and the housing, which surrounds the inflector electrodes, are also shown. Only the portion of the housing below the median plane is shown for a better visualization.

collimator has been designed at 10 mm from the inflector entrance to reduce the electric fringe field effect. It has a circular shape with an internal hole of radius equal to 6 mm. In addition, the aspect ratio between the width and the distance between the inflector electrodes was chosen to be 2.5. A tilt parameter [9] $k' = -1$ is needed to centre the beam. The 3D view of the spiral inflector with its collimator and housing, as developed for the IsoDAR test bench cyclotron, is presented in fig. 3. Only the portion of the housing below the median plane is shown for a better visualization.

Table II contains the spiral inflector and collimator parameters.

Due to the high beam current to be injected, a 14 mm constant gap between the inflector electrodes has been adopted. The large-gap spiral inflector has to deal with the small available space and high injection energy of the beam. This implies a high voltage to be applied on the inflector electrodes ($\pm$ 18.88 kV) to bend the beam onto the median plane. Further investigations on the engineering and machining process of the electrostatic device are foreseen to provide indications about the maximum voltage to be applied to the inflector electrodes.

3. – Beam dynamics simulations

The orbit tracking in the cyclotron has been performed by means of the AOC code, developed by IBA for different applications in the context of medical and industrial accelerators. It enables to calculate particle trajectories as a function of time, including space charge. In addition, simulations of the 3D design orbit of the cyclotron spiral inflector in the varying 3D magnetic field have been made and the electric fringing field effects at the inflector entrance and exit have been taken into account. More details about the AOC code can be found in ref. [12].

We simulated the reference orbit motion starting from a point along the axial injection line placed at 100 mm from the median plane, about 20 mm from the collimator entrance. The initial RF phase of the reference orbit was chosen in order to optimize the horizontal

TABLE II. – *Spiral inflector and collimator parameters.*

Electric bending radius	50 mm	Inflector lenght	79.7 mm
Tilt parameter	−1	Aspect ratio	2.5
Constant gap	14 mm	Electrodes voltage	± 18.88 kV
Collimator internal radius	6 mm	Collimator external radius	14 mm
Collimator thickness	16 mm	Collimator-inflector distance	10 mm

orbit centering, energy gain per turn and vertical excursion in the cyclotron centre.

The designed spiral inflector and central region allow a good injection and first turns acceleration of the reference orbit in the test bench cyclotron, as shown in figs. 4 and 5. Figure 4(a) shows the z coordinate of the spiral inflector centroid curve *versus* the number of turns. The zoom of the plot in the region near the median plane ($z = 0$ mm) is highlighted in fig. 4(b). At the inflector exit, the centroid curve is perfectly onto the median plane and its vertical momentum is near to zero. Figure 5(a) presents the x-y plane projection of the reference orbit tracked in the whole injection system. The circles and crosses give the particle positions when the dee voltage is zero or maximum respectively. The positioning of the circles along the dee centerline and of the crosses along the gap centerline is a clear indication of a good isochronism (see also fig. 2). In addition, the same plot shows a good horizontal centering of the reference orbit with respect to the cyclotron centre. The plot in fig. 5(b) shows that the maximum vertical excursion of the reference orbit from the median plane is very small, lower than 0.2 mm, along the whole path in the central region. The region near the median plane is shown for a better visualization.

Once optimized the injection system design for the reference orbit, first investigations on the beam behaviour have been carried out. We simulated the motion of a particles bunch from the same starting point considered for the reference orbit up to the last turn in the accelerating machine. For this purpose, 5000 particles with a uniform distribution

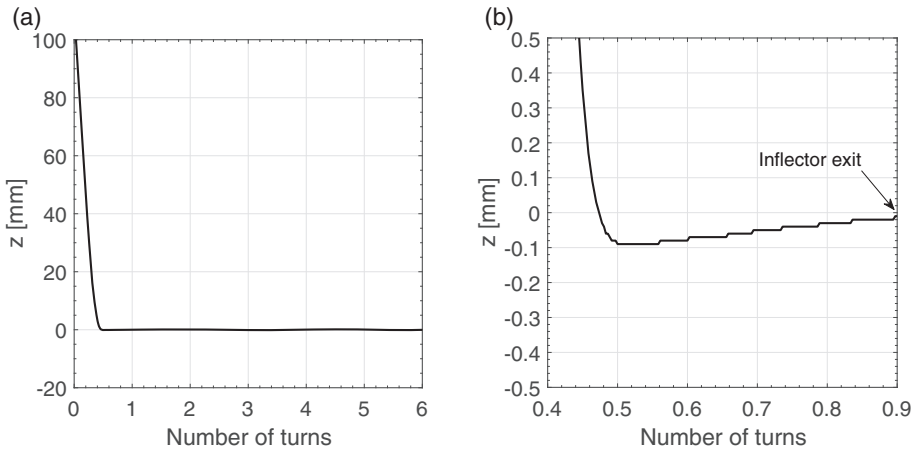

Fig. 4. – On the left, vertical coordinate of the spiral inflector centroid curve. On the right, zoom of the plot in the region near the median plane (z = 0 mm).

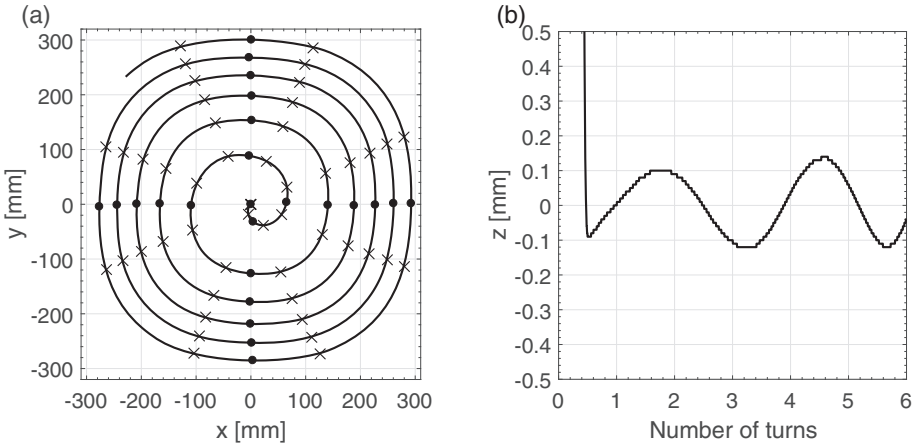

Fig. 5. – On the left, the x-y plane projection of the reference orbit in the whole injection system. The circles and crosses indicate the particle positions when the dee voltage is zero or maximum respectively. On the right, vertical coordinate of the reference orbit along the whole path in the central region. The region near the median plane is shown for a better visualization.

in both the x-x' and y-y' phase spaces were taken. We used a normalized emittance of 1 π·mm·mrad, which is about 20% larger than the expected beam emittance delivered by the RFQ. A round beam having half beam size equal to 5 mm has been considered. More details about the beam parameters are listed in table III. In addition, an energy spread equal to ± 2% of the injection energy value was adopted. An average beam current of 5 mA and various bunch lengths (30°, 20°, 10°, 5°) were simulated to investigate the space charge effects.

Beam transmission and losses in the central region were evaluated in the presence and absence of space charge for all considered bunch lengths (see table IV). The losses are localized in the cyclotron centre, especially at the inflector exit and in the first half turn, due to the beam vertical envelope size that exceeds the small vertical aperture of the housing hole and dee-tips (fig. 6(a)). The growth of beam emittance through the spiral inflector and the transverse defocusing of the beam at the inflector exit are the main responsibles of losses. The factors that could contribute to a larger emittance growth through the spiral inflector are: a) 6D phase space strongly correlated by the spiral inflector optics; b) large tilt parameter k' (strong transfer coupling); c) not optimized beam properties before the inflector entrance. Also the space charge effects lead to the emittance growth through the spiral inflector and transverse defocusing at the inflector exit. Indeed, for the bunch length equal to 30°, corresponding to the RF phase acceptance of the central region, the transmission is lower when the space charge is taken into account.

TABLE III. – *Beam parameters.*

x, y	5 mm	x', y'	53 mrad	$\epsilon_{n,x}, \epsilon_{n,y}$	1 $\pi \cdot$ mm $\cdot$ mrad	ϵ_x, ϵ_y	115 $\pi \cdot$ mm $\cdot$ mrad
r_{12}	-0.9	α_x, α_x	2.065	β_x, β_y	0.217 m	γ_x, γ_y	24.259 m^{-1}

TABLE IV. – *Beam transmission and losses in the central region evaluated in presence and absence of space charge and for different bunch lengths.*

	Bunch length	Losses	Transmission
$\langle I \rangle = 0\,mA$	30°	645 particles	87.1%
$\langle I \rangle = 5\,mA$	30°	1667 particles	66.7%
$\langle I \rangle = 5\,mA$	20°	1891 particles	62.2%
$\langle I \rangle = 5\,mA$	10°	2216 particles	55.7%
$\langle I \rangle = 5\,mA$	5°	2414 particles	51.7%

In addition, in the presence of space charge, the losses increase as the bunch length reduces. This can be explained with the decreasing of the particles distance and, consequently, the increase of the electrical repulsive forces, resulting in the beam transverse defocusing in the cyclotron centre.

Particular attention has been also paid to the beam radial size. As for the beam transmission, it has been evaluated in the presence and absence of space charge and for all bunch lengths listed in table IV. Unfortunately, turn separation has not been observed in all cases, also for small bunch length. Figure 6(b) shows the simulation of beam motion in the designed injection system in the presence of space charge and for a bunch length equal to 5°. As one can see, the beam radial size along the whole path in the cyclotron does not allow to have turn separation. From a space charge point of view, a short bunch length would help to obtain the turn separation. Indeed, the space charge effects induce a vortex motion [14]. After more turns in the machine, a round beam emerges with an intense core, surrounded by a halo. The halo size is dependent on the initial bunch length. If the bunch length is short, a small halo develops and, consequently,

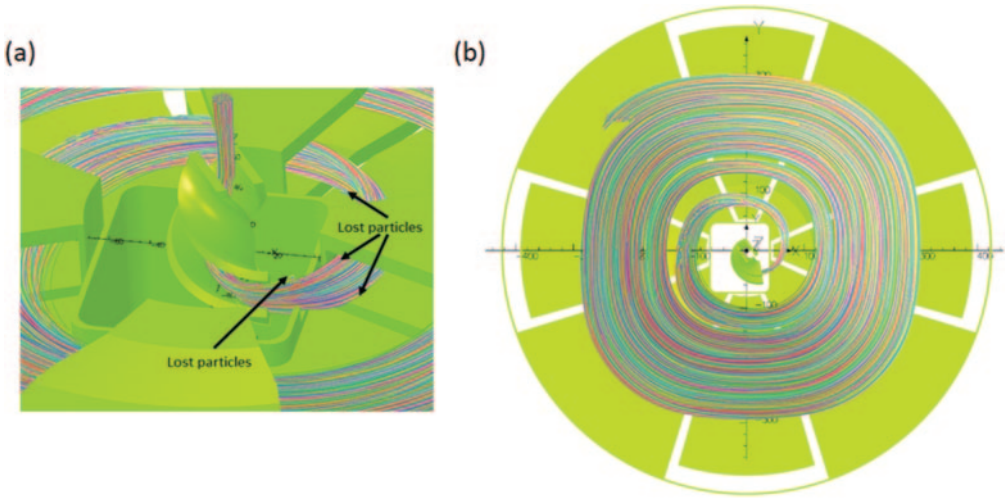

Fig. 6. – On the left, simulation of the axially injected beam through the spiral inflector into the IsoDAR test bench cyclotron. Losses are localized in the cyclotron centre, especially at the inflector exit and in the first half turn in the machine. On the rigth, the x-y plane projection of the beam motion in the whole injection system in the presence of space charge and for a bunch length is equal to 5°.

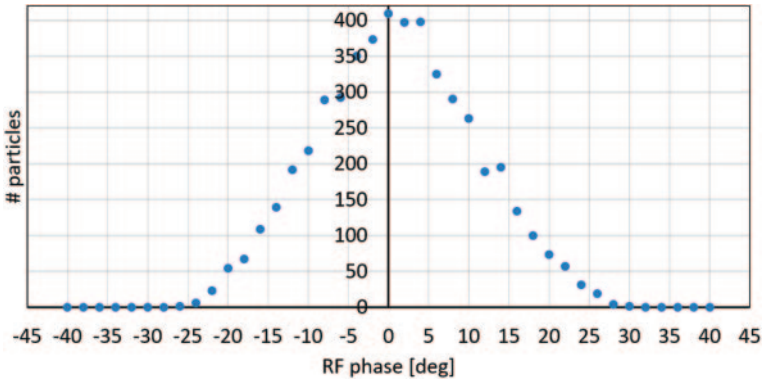

Fig. 7. – Distribution of the RF phase of the beam particles around the reference RF phase at the inflector exit.

the overlap between the radial beam envelopes of adjacent turns is avoided. A possible cause of the missing turn separation, also for small bunch lengths, is the RF phase bunch broadening, due to the spiral inflector. This means that the bunch length increases when particles move through the spiral inflector. A simulation has been performed to verify the effect of the spiral inflector on the RF phase bunch length. For the sake of simplicity, we assumed absence of space charge and the same energy and RF phase values for all beam particles. The starting position already considered for the reference orbit and the beam emittance properties listed in table III have been considered. Figure 7 shows that the RF phase broadening introduced by the spiral inflector is about $\pm$ 25°.

Actually, the bunch length at the inflector exit should be even greater because also the beam motion in the drift between the RFQ and the spiral inflector ($\approx$ 20 cm) contribuites to the RF phase broadening. Further investigations are mandatory to find out if further effects contribute to destroy the turn separation.

4. – Conclusions

The space charge effects are a limitating factor in the injection into the IsoDAR cyclotron through a spiral inflector and in the acceleration in the cyclotron centre. The design of the IsoDAR injection system requires precise numerical calculations and many iterations before good beam centering, vertical focusing and longitudinal matching are obtained. The current injection system design is not able to guarantee the required turn separation. A possible cause is the spiral inflector, which introduces a RF phase spread effect. In addition, particle losses are verified in the cyclotron centre due to the emittance growth through the spiral inflector and transverse defocusing at the inflector exit. This study allows us to understand how different effects influence the beam dynamics in the injection system, both in the spiral inflector and in the central region. We foresee a further refinement of the simulations, with the aim of improving the injection system design, in particular looking at the orbit turn separation, transmission, beam size and energy spread. It will be important to enlarge the 3D model of the test bench cyclotron to study more realistically the space charge effects, also looking at the whole accelerating process in the IsoDAR machine and not only at the few turns realizable in the test bench cyclotron. Furthermore, since the characteristics of the beam at the cyclotron

injection depend on the focusing element placed before it, a comprehensive simulation of the cyclotron injection cannot exclude the RFQ, currently in the design phase. Therefore, in the next months further efforts will be needed to include coherently the RFQ within the simulations.

* * *

Special thanks to Luciano Calabretta for his support during the present study. This work was performed at IBA company. I would like to thank all members of the R&D group of the company for their support during the study. In particular, I would like to extend my sincere gratitude to Eric Forton for giving me the opportunity to perform an intership at IBA and Willem Kleeven for his support and valuable suggestions during my stay in the company.

REFERENCES

[1] Bungau A. *et al.*, *Phys. Rev. Lett.*, **109** (2012) 141802.
[2] Conrad J. M. *et al.*, *Phys. Rev. D*, **89** (2014) 072010.
[3] Abs M. *et al.*, (2015) arXiv:1511.05130.
[4] Castro G. *et al.*, *Rev. Sci. Instrum.*, **87** (2016) 083303.
[5] Xu Y. *et al.*, *Rev. Sci. Instrum.*, **85** (2014) 02A943.
[6] Axani S. *et al.*, *Rev. Sci. Instrum.*, **87** (2016) 02B704.
[7] Axani S. N., *PoS*, **ICHEP2016** (2017) 484.
[8] Winklehner D. *et al.*, *Rev. Sci. Instrum.*, **87** (2016) 02B929.
[9] Belmont J. L. and Pabot J. L., *IEEE Trans. Nucl. Sci.*, **NS-13** (1966) 191.
[10] Kleeven W., *Injection and extraction for cyclotrons*, in *Proceedings of CERN Accelerator School, Small accelerators*, edited by Brandt D. (CERN, Geneva) 2006, pp. 271–296.
[11] Kleeven W., *Some examples of recent progress of beam-dynamics studies for cyclotrons*, in *Proceedings of the 21st International Conference on Cyclotrons and their Applications, Zurich, Switzerland, 2016, WEA01* (JACoW) 2016, pp. 244–250.
[12] Kleeven W. *et al.* , *AOC, a beam dynamics design code for medical and industrial accelerators at IBA*, in *Proceedings of the 7th International Particle Accelerator Conference, Busan, Korea, 2016, TUPOY002* (JACoW) 2016, pp. 1902–1904.
[13] Cobham, `http://operafea.com`.
[14] Adam S., *Space charge effects in cyclotrons - From simulations to insights*, in *Proceedings of the 14th International Conference on Cyclotrons and their Applications, Cape Town, South Africa, 1995, H03* (JACoW) 1995, pp. 446–449.